

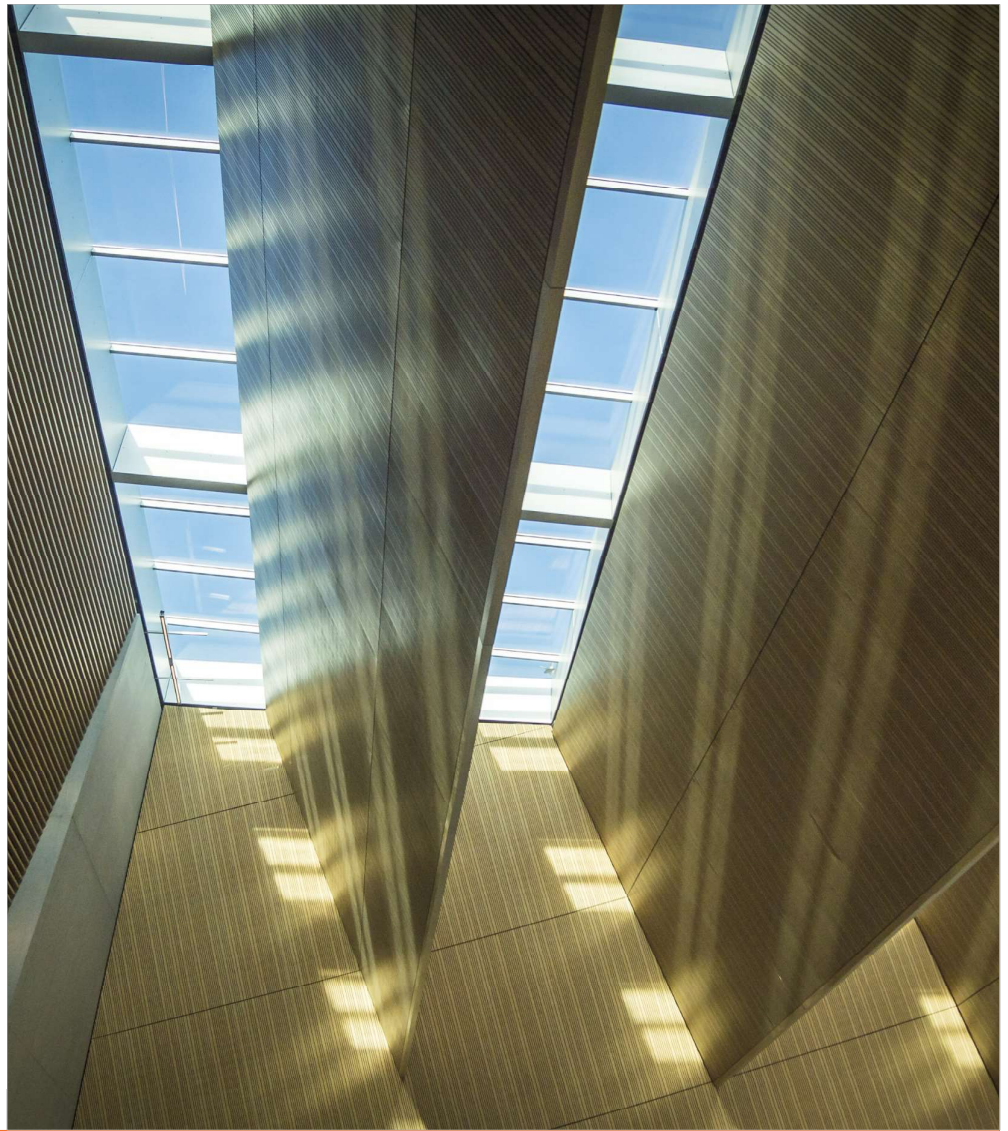
ECCM

20

26-30 JUNE

2022

LAUSANNE
SWITZERLAND



Proceedings of the 20th European Conference on Composite Materials

COMPOSITES MEET SUSTAINABILITY

Vol 1 – Materials

Editors : Anastasios P. Vassilopoulos, Véronique Michaud

Organized by :

EPFL

Under the patronage of :

CCLAB
Composite
Construction
Laboratory

LPAC
Laboratory for Processing
of Advanced Composites

ESCM
EUROPEAN SOCIETY
FOR COMPOSITE MATERIALS

**Proceedings of the 20th
European Conference on Composite Materials
ECCM20
26-30 June 2022,
EPFL Lausanne Switzerland**

Edited By :

Prof. Anastasios P. Vassilopoulos, CCLab/EPFL

Prof. Véronique Michaud, LPAC/EPFL

Organized by:

Composite Construction Laboratory (CCLab)

Laboratory for Processing of Advanced Composites (LPAC)

Ecole Polytechnique Fédérale de Lausanne (EPFL)

Published by :

Composite Construction Laboratory (CCLab)
Ecole Polytechnique Fédérale de Lausanne (EPFL)
BP 2225 (Bâtiment BP), Station 16
1015, Lausanne, Switzerland

<https://cclab.epfl.ch>

Laboratory for Processing of Advanced Composites (LPAC)
Ecole Polytechnique Fédérale de Lausanne (EPFL)
MXG 139 (Bâtiment MXG), Station 12
1015, Lausanne, Switzerland

<https://lpac.epfl.ch>

Cover:

Swiss Tech Convention Center
© Edouard Venceslau - CompuWeb SA

Cover Design:

Composite Construction Laboratory (CCLab)
Ecole Polytechnique Fédérale de Lausanne (EPFL)
Lausanne, Switzerland

©2022 ECCM20/The publishers

The Proceedings are published under the CC BY-NC 4.0 license in electronic format only, by the Publishers.

The CC BY-NC 4.0 license permits non-commercial reuse, transformation, distribution, and reproduction in any medium, provided the original work is properly cited. For commercial reuse, please contact the authors. For further details please read the full legal code at <http://creativecommons.org/licenses/by-nc/4.0/legalcode>

The Authors retain every other right, including the right to publish or republish the article, in all forms and media, to reuse all or part of the article in future works of their own, such as lectures, press releases, reviews, and books for both commercial and non-commercial purposes.

Disclaimer:

The ECCM20 organizing committee and the Editors of these proceedings assume no responsibility or liability for the content, statements and opinions expressed by the authors in their corresponding publication.

Editorial

This collection gathers all the articles that were submitted and presented at the 20th European Conference on Composite Materials (ECCM20) which took place in Lausanne, Switzerland, June 26-30, 2022.

ECCM20 is the 20th edition of a conference series having its roots back in time, organized each two years by members of the European Society of Composite Materials (ESCM).

The ECCM20 event was organized by the Composite Construction laboratory (CCLab) and the Laboratory for Processing of Advanced Composites (LPAC) of the Ecole Polytechnique Fédérale de Lausanne (EPFL).

The Conference Theme this year was “Composites meet Sustainability”. As a result, even if all topics related to composite processing, properties and applications have been covered, sustainability aspects were highlighted with specific lectures, roundtables and sessions on a range of topics, from bio-based composites to energy efficiency in materials production and use phases, as well as end-of-life scenarios and recycling.

More than 1000 participants shared their recent research results and participated to fruitful discussions during the five conference days, while they contributed more than 850 papers which form the six volumes of the conference proceedings. Each volume gathers contributions on specific topics:

Vol 1 – Materials

Vol 2 – Manufacturing

Vol 3 – Characterization

Vol 4 – Modeling and Prediction

Vol 5 – Applications and Structures

Vol 6 – Life Cycle Assessment

We enjoyed the event; we had the chance to meet each other in person again, shake hands, hold friendly talks, and maintain our long-lasting collaborations. We appreciated the high level of the research presented at the conference and the quality of the submissions that are now collected in these six volumes. We hope that everyone interested in the status of the European Composites’ research in 2022 will be fascinated by this publication.

The Conference Chairs

Anastasios P. Vassilopoulos, Véronique Michaud

Hosting Organizations

Composite Construction Laboratory (CCLab)
Laboratory for Processing of Advanced Composites (LPAC)
Ecole Polytechnique Fédérale de Lausanne (EPFL)

Venue

Swiss Tech Convention Center (<https://www.stcc.ch>)

Conference Chairs

Chair : Prof. Anastasios P. Vassilopoulos, EPFL, Switzerland
Co-Chair: Prof Véronique Michaud, EPFL, Switzerland

International Scientific Committee

Prof. Malin Åkermo SE	Prof. Theodoros Loutas GR
Dr. Emmanuel Baranger FR	Prof. Veronique Michaud CH
Prof. Christophe Binetruy FR	Prof. Alessandro Pegoretti IT
Prof. Pedro Camanho PT	Prof. Joao Ramoa Correia PT
Prof. Konstantinos Dassios GR	Prof. Jose Sena-Cruz PT
Prof. Brian Falzon UK	Prof. Antonio T. Marques PT
Prof. Kristofer Gamstedt SE	Prof. Thanasis Triantafillou GR
Prof. Sotiris Grammatikos NO	Prof. Albert Turon ES
Prof. Christian Hochard FR	Prof. Anastasios P. Vassilopoulos CH
Prof. Marcin Kozlowski PL	Prof. Martin Fagerström SE
Prof. Stepan Lomov BE	Dr. Alexandros Antoniou DE
Dr. David May DE	Prof. Lars Berglund SE
Prof. Stephen Ogin UK	Prof. Michal Budzik DK
Prof. Gerald Pinter AT	Prof. Lucas Da Silva PT
Prof. Silvestre Pinho UK	Dr. Andreas Endruweit UK
Prof. Yentl Swolfs BE	Prof. Mariaenrica Frigione IT
Dr. Julie Teuwen NL	Dr. Larissa Gorbatikh BE
Dr. Panayota Tsotra CH	Dr. Martin Hirsekorn FR
Prof. Wim van Paepegem BE	Prof. Vassilis Kostopoulos GR
Prof. Dimitrios Zarouchas NL	Prof. Jacques Lamon FR
Dr. Andrey Anishevich LV	Prof. Staffan Lundstrom SE
Prof. Christian Berggreen DK	Prof. Peter Mitschang DE
Dr. Nicolas Boyard FR	Dr. Soraia Pimenta UK
Prof. Valter Carvelli IT	Prof. Paul Robinson UK
Prof. Klaus Drechsler DE	Dr. Olesja Starkova LT
Prof. Bodo Fiedler DE	Prof. Sofia Teixeira de Freitas NL
Dr. Nathalie Godin FR	Dr. Stavros Tsantzalis GR
Prof. Roland Hinterholz AT	Prof. Danny van Hemelrijck BE
Prof. Ian Kinloch UK	Prof. Michele Zappalorto IT
Dr. Thomas Kruse DE	Dr. Miroslav Cerny CZ

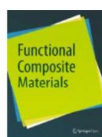
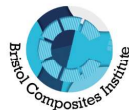
Local Organizing Committee

Prof. Anastasios P. Vassilopoulos, EPFL
Prof. Véronique Michaud, EPFL

Angélique Crettenand and Mirjam Kiener, Lausanne Tourisme

And all those who helped, colleagues who reviewed abstracts and chaired sessions, and CCLab and LPAC students and collaborators who worked hard to make this conference a success.

Sponsors



Supporting partners



Contents

Contribution to the determination of thermal and chemical residual stresses in fiber reinforced composites using the incremental hole drilling method: numerical and experimental approach	1
A novel bio-inspired microstructure for progressive compressive failure in multidirectional composite laminates	7
Fluorescent marking of fibre reinforced plastic for component and material identification in the context of material flow canalization	14
Electrofusion welding of thermoplastic composite pipes	22
Mechanical characterisation of a long discontinuous fibre reinforced composite to evaluate the recycling potential of carbon fibre in structures	29
The mass production of MWCNTS/epoxy scaffolds using lateral belt-driven multi-nozzle electrospinning setup to enhance physical and mechanical properties of CFRP	37
Thermo-mechanical modelling of UD composites to investigate self-heating and thermal softening effect of polymer matrix	43
Towards the development of LDPE multi-layered packaging films with enhanced bioactivity	51
Investigation of 3D printed polymers and moulded composites in hot concentrated acid	59
The effect of resorcinol bis(diphenyl phosphate) on the flammability and flexibility of flame retarded epoxy gelcoats	67
Carbon and glass SMC hybrids in a sandwich arrangement	75
Investigating the effect of interface angle and ply thickness on mode II delamination behaviour of carbon/epoxy laminated composites	82
Ranking the influence of key uncertainties in the curing of thermoset laminates	90
Investigation of the mechanical properties of fuzzy CNT and CNT/CNC integrated glass fiber/epoxy composites with different reinforcing strategies	98
Mechanical properties of epoxy/carbon fiber composite fabricated by filament winding under monotonic and fatigue loadings	106
Thermoset polymer scaling effects in the microbond test	114
Ply orientation effects in multidirectional carbon/epoxy open-hole specimens subjected to shear loading	122
Carbon fibre foams: internal structure and mechanical properties	128
Study on the mode I fracture toughness of composite laminates based on the correlation between AE signal and crack front shape	136
The influence of production wastes incorporation on the properties of thermoplastic matrices	144
Extended failure models for global and local analyses of composite aerostructures	152
High strain rate characterization of twill woven carbon-polyamide laminate in longitudinal compression	160
Damage characterisation in open-hole composites using acoustic emission and finite element, validated by x-ray ct	167

An investigation on the mechanical properties of SPCS	175
Hybrid testing for composite substructures	183
Mechanical characterization of 3R-repairable composites and 3R bonding techniques produced by different processes and their repair efficiency	188
A study to improve the efficiency of laminated heating module for electric vehicles	195
Flexural behaviour of polyurethane foam filled high performance 3-d woven i-beam composites	203
Second life for aeronautical manufacturing materials	211
Development of flame retardant coatings for e-caprolactam-based polyamide 6 composites	217
Development of a carbon fiber reinforced sheet molding compound for high temperature applications	225
Development of electric vehicle underbody shield using carbon fiber/poly(ethylene terephthalate) and self reinforced polypropylene composites	233
Sustainable epoxy thermosets with potential applications in the aerospace sector	241
The influence of temperature and matrix chemistry on interfacial shear strength in glass fibre epoxy composites	249
Ceramic spatial structures as a new method of reinforcing ferrous alloys	257
Low velocity impact and residual tensile and compressive strength analysis of carbon fibre SMC composites	263
Influence of TEX linear density on mechanical properties of 3D woven i-beam composites	271
Effect of fiber microstructure on kinking in unidirectional fiber reinforced composites imaged in real time under axial compression	279
Effect of heat/fire on structural damage to carbon fibres in carbon fibre-reinforced composites	287
Use of carbon particles in fiber/epoxy UD laminates	294
Validation of composite aerostructures through integrated multi-scale modelling and high-fidelity sub-structure testing facilitated by design of experiments and BAYESIAN learning	302
Easy-repairing of high performance fibre reinforced composites with multiple healing cycles and integrated damage sensing	306
The effect of short carbon fibers on viscoelastic behavior of UHMWPE	314
Development of polypropylene melt-blown fine fiber interleaved single-polypropylene composites	322
Tailored out-of-oven curing of high performance FRPS utilising a double positive temperature coefficient effect	330
Remote activation of frontal polymerization for sustainable manufacturing of thermosets and composites	337
Sustainable multifunctional composites: from energy efficient manufacturing to integrated sensing and de-icing capabilities	344
Improved energy absorption of novel hybrid configurations under static indentation	348
Influence of brazier effect on GFRP thin circular cylinder - an experimental and numerical study	354

Multiscale interface behaviour and performance of GF-pc composite	362
Two-dimensional mode II delamination growth in composite laminates with in-plane isotropy . . .	371
Effect of lightweight fillers on the properties of polymer concrete	379
Non linear elastic behaviour of CFRP plies: material or geometrical feature?	387
Evaluation of the shear behavior of PETG/cf and pc/cf coupons manufactured using large-scale additive manufacturing processes	393
3D-print path generation of curvilinear fiber-reinforced polymers based on biological pattern forming	401
Synchrotron radiation 3D computed tomography study on in-situ mechanical damage progression of nanoengineered glass fiber reinforced composite laminates with integrated multifunctionality . . .	408
INSIGHT on induction welding of reactive PMMA carbon fiber composites	415
Litz wire-based multifunctional composites for managing thermal and mechanical loads within electrical systems	423
Shift factor dependence on physical aging and temperature for viscoelastic response of polymers . .	431
Characterization of novel sustainable composite materials based on ELIUM® 188 o resin reinforced with a Colombian natural fiber	439
Combined DIC-infrared thermography for high strain rate testing of composites	447
Effect of gap defects on in-situ AFP-manufactured structures	455
Polypropylene/flax fabric composite laminates: effects of plasma and thermal pre-treatments of reinforcing fibres	463
Improving the delamination bridging behaviour of z-pins through material selection	471
Study on the effect of strain rate and temperature on the mechanical behavior of polypropylene-glass fiber compound and thermoplastic olefin	479
Simultaneous spinning of recycled thermoplastics and glass fibers for hybrid yarns used in sustainable composites	486
Reprocessable vitrimer composites	493
Characterizing the tensile and compressive behavior of PETG/cf and pc/cf manufactured using large scale additive processes	501
Influence of mechanical properties of matrix on bending strength of uni-directional vinyl ester composite	509
Strain sensing of complex shaped 3D woven composites using MXENE nanoparticles	516
Comparison of the fire reaction of a carbon-epoxy composite at small scale and large tests	522
Efficient and versatile 3D woven composite manufacturing: novel approaches on the quality of composite fabrication	532
Electrical conductivity as an instrument for damage diagnostic of nanomodified glass fiber reinforced plastic	539
Out-of-oven manufacturing for natural fibre composites with integrated deformation and degradation sensing	547

Controlling electrical percolation in thermoplastic composites through informed selection of fillers	555
Macroscale magnetic alignment of multiple discontinuous ferromagnetic fibres in a polymer matrix	563
Laser-induced graphene carbon fiber reinforced composites for multifunctionality	569
Influence of fibre/matrix interface on gas permeability properties of CF/PVDF composites	577
Tribological study on wood and graphene reinforced high density polyethylene	585
Structural health monitoring (SHM) on fibre reinforced composite t-joint geometry manufactured by a novel 3R resin	593
The use of recycled materials towards sustainability: biocomposites manufactured in melt compounding	600
Fully bio-based epoxy-amine resins from circular economy: conception, multiscale structural and mechanical behaviour characterization toward low carbon-footprint composites	608
Mechanism-based assessment of cellulose-based biocomposite cottonid for sustainable construction	616
Novel cellulose based composite material for thermoplastic processing	624
Towards more efficient and environmental friendly flax-based eco-composite through direct F2 fluorination as a compatibilization treatment	632
Flax fibre sizings for fibre-reinforced thermosets - investigating the influences of different sizing agents on fibre moisture content and composite properties	640
Elaboration of hybrid bio-composites with thermoplastic matrix: material formulation and modelling of the quasi-static behaviour	648
Converting recycled glass fibre and polypropylene to feedstock (filament) for material extrusion additive manufacturing	656
Turning oil palm waste into all-cellulose fibreboards utilising refined pulp fibres	662
Soft composites from bio-based resources	668
All lignocellulose biocomposites for woody like materials	675
Dilatometric and fracture mechanism investigations on poly (lactic acid) PLA-calcium carbonate biocomposites	681
Effect of fibrillation of flax mat binder on the impact response of unidirectional flax/epoxy composites and comparison with a glass/epoxy composite	689
Morphological image analysis: a candid technique to determine density and geometric shapes of bio-based fibers and permanent damage due to interaction with water molecules	697
Cost-effective hemp staple fibre yarns for high-performance composite applications	705
Influence of wet/dry cycling on mechanical properties of hemp-reinforced biocomposites	713
Biodegradable polymer films to prevent biofilm formation for food packaging application	721
Life cycle assessment of natural fibre reinforced polymer composites	727
Development of quasi-unidirectional woven fabrics with 100% hemp rovings for composite materials applications	735

Effect of different natural fibres on mechanical and disintegration properties of compostable biobased plastics	743
High-strength rigid boards made from industrially produced bacterial cellulose	750
Manufacturing and mechanical characterisation of unidirectional fique fibres reinforced polypropylene composites	758
Behaviour and repair of flax/ELIUM biocomposites loaded in low velocity impact	766
On the flexural strength and actuation of wood branches – mechanisms useful in composite design?	773
Mechanical modelling of viscoelastic hierarchical suture joints and their optimization and auxeticity	779
Biobased glass fiber sizings for composites in medical and technical applications	788
The effect of humidity on the mechanical properties of flax-polyester biocomposites with different fibre architectures	795
Functionalized wood composites for mechanical energy harvesting and vibration sensing	801
Development of bio-based CFRP laminates for strengthening civil engineering structures	807
Bio-based vacuum infused glass fibre reinforced unsaturated polyester composites for high-performance structural applications	815
Hygrothermal ageing of a GFRP composite produced by vacuum infusion with a novel bio-based unsaturated polyester resin	823
Towards adhesives-free bio-based composites via UV-assisted interfacial cross-linking	831
Towards integrated health monitoring of bio-based composite structures: influence of acoustic emission sensor embedment on material integrity	838
The emerging era of visionary composites by plant-grown matrix and reinforcing fibres: the cellular adhesion	847
Lemongrass plant leaf and culm as potential sources of reinforcement for bio-composites	855
A novel method to quantify self-healing capabilities of fibre reinforced polymers	863
Enabling reparability and reuse of epoxy composites: epoxy vitrimers	871
Low velocity impact response and post impact assessment of healable CFRPS modified with diels-alder resin applied by melt electro-writing process	879
Evaluation of the self-healing capability of a polycaprolactone functionalized interphase for polymer composite applications	887
Highly conductive polypropylene based composites for bipolar plates for polymer electrolyte membrane fuel cells	894
Conductive smart nanocomposite materials for structural health monitoring and motion detection .	901
The effect of conductive network on positive temperature coefficient behaviour for multifunctional composites: from flexible sensing to sustainable manufacturing	909
Graphite filled thermoplastics for thermally conductive pipes	917
Recycling of graphitic bipolar plates for vanadium redox batteries	925

Damage sensing based on electrically conductive nanoparticles in sandwich-structured composites	933
A novel lightning strike protection system comprising an all-polymeric conductive resin	939
Low temperature growth of carbon nanotubes on fibers using copper as catalyst	945
Effect of nanoarchitecture on EMI shielding properties of nanocomposites at high content of graphite nanoplatelets	953
Rapid and facile preparation of multifunctional BUCKYPAPER nanocomposite films	961
Investigation of the thermal and mechanical properties of composite materials with amine-functionalized reduced graphene oxide inclusions	967
The application of coated carbon nanotubes in lightweight metal matrix composites	975
Nanoparticle reinforced lightweight metal composites	981
Self-assembly of NBR and NOMEX via electrospinning: rubbery NANOFIBERS for improving CFRP delamination resistance	986
Chemical compatibilizers as an approach to improve the mechanical properties of poly(propylene) reinforced with graphene nanoplatelets	994
Piezoresistivity of nanocomposites: accounting for CNT contact configuration changes	1002
Ionic polydimethylsiloxane-silica nanocomposites: from synthesis and characterization to self-healing property	1010
Mechanical behaviour of ultrathin carbon nanomembranes for water purification	1018
Intense pulsed light welding process with simultaneous mechanical roll-pressing for highly conductive silver nanowire/polyethylene terephthalate composites	1025
Surface functionalization of quartz fibres by direct growth of carbon nanostructures	1032
Characterisation of graphene-enhanced carbon-fibre/PEEK manufactured using spray-deposition and laser-assisted automated tape placement	1040
High speed imaging of the ultrasonic deagglomeration of nanoparticles in water	1048
Effects of microwave-assisted cross-linking on the creep resistance and measurement accuracy of the coaxial-structured fiber strain sensor	1056
Mechanics of reinforcement of polymer-based nanocomposites by 2D materials	1062
Enhanced mechanical properties of hierarchical MXENE/cf composites via low content electrophoretic deposition	1069
Remote field induced response of polymer nanocomposites embedded with surface-functionalised dielectric nanoparticles	1079
Effects of hybridization and ply thickness on carbon/carbon composite laminates strength and toughness	1091
Effect of weathering on the long-term performance of natural fiber reinforced recyclable polymer composites for structural applications	1097
Fibres hybridization for thermoplastic matrix composites	1104
Mechanical characterization of a three-dimensional hybrid woven composites	1112

Design and characterization of tough architected ceramic-based composites	1119
Bearing strength high performance fibre metal thin-ply laminates	1127
Visoelastic and VISCOPLASTIC creep modelling of short-glass fibre reinforced polypropylene composites	1130
3D printed short carbon fibres reinforced polyamide: tensile and compressive characterisation and multiscale failure analysis	1137
Estimation of interfacial shear strength of long glass fibre composites by x-ray computed tomography	1145
Material characterisation and fatigue data correlation of short fibre composites: effect of thickness, load ratio and fibre orientation at elevated temperature	1151
Local stress-strain behaviour in short glass fibre reinforced polymers - a comparison of different simulation approaches with experimental results based on x-ray computed tomography data	1159
Effect of fibre orientation, temperature, moisture content and strain rate on the tensile behaviour of short glass fibre-reinforced polyamide 6	1167
A mode II testing method for hybrid composites	1175
Deployable composite meshes – modelling, manufacture and characterisation	1183
Are pseudo-ductile all-carbon hybrid laminates notch insensitive in open hole tension?	1191
Reparability as a new function for high-performance pseudo-ductile hybrid composites	1197
On the optimal design of smart composite sensors for impact damage detection	1205
Impact properties of flax-carbon hybrid composites under low-velocity impact	1213
Enhancement of thin-ply composites translaminar toughness through fiber-hybridization: towards a discrimination with the ply thickness effect?	1220
Assessing the impact behavior of highly aligned fiber hybrid composites	1228
Development and characterization of hybrid thin-ply composite materials	1236
Tensile fatigue performance of carbon-carbon hybrid quasi-isotropic laminate	1244
Variable stiffness lattice structures	1251
Virtual-physical engineering of a graded CFRP/titanium aircraft suspension strut	1258
Manufacturing and properties of hybrid composites of continuous steel and glass fibers made by tailored fiber placement	1266
A novel hybrid thermoset-thermoplastic robot-based production concept for lightweight structural parts: a special view on the hybrid interface	1274
Tensile properties of deep drawn in-situ polymerized fiber-metal-laminates	1282
Micro-scale modelling of composites made of RCF/ PA6 staple fiber yarns with special emphasis on fiber length distribution	1290
Micro-ct based assessment of 3D braided AL2O3 reinforcement uniformity and permeability of all-oxide ceramic matrix composites production processes	1296
Multi-scale modeling of the thermo-viscoelastic behavior of 3D woven composites	1303

Advanced natural fibre textiles for composite reinforcement	1311
Characterization of interlock 3D permeability tensor for c-RTM process	1318
Automated g-code to FE mesh conversion - modelling polymer penetration into a textile to generate a polymer-textile composite made by additive manufacturing	1326
Micro-ct-based numerical validation of the local permeability map for the b-pillar infusion simulation	1333
Effect of temperature on damage onset in three-dimensional (3D) woven organic matrix composites for aero-engines applications	1341
Simulation of frictional contact interactions within jacquard harness of weaving looms for 3D interlock fabrics	1349
Laccase-enzyme treatment of flax fibres for improved interfacial strength in natural fibre composites	1357
DIC-based monitoring on DEBONDING crack propagation in wrapped composite joints	1362
Ultrasoft and hyperelastic electrically conductive nanocomposites for strain sensing applications . .	1369
Mechanical, rheological and thermal evaluation of poly(lactic acid) (PLA) / micro fibrillated cellulose (MFC) plasticized biocomposites produced with flat die extrusion and calendaring	1377
Optimization of an exoskeleton	1384
Banana fibre as sustainable and renewable resource for reinforcement of polylactic acid	1391
Hybrid ratio effect on flexural properties for CFRP-natural fiber composite hybrid materials	1398
Investigation of energy absorption capacity of novel 3D-printed glass fibre reinforced thermoplastic bio-inspired structures	1404
Rapid fatigue life prediction of CFRP laminates by combining the data of self-heating with stiffness degradation	1412
Performance evaluation of e-skin for structural deformation detection	1420
Temperature detectable surface coating and self-sensing system with carbon nano-tube/epoxy composites	1426
Solubility behavior of graphene-oxide with various solvents	1433
Biodegradable polymer-based composites filled with biochar for tunable release of carvacrol	1437
Designing bicontinuous silica-epoxy nanocomposites	1445
Robust continuous production of carbon nanotube-grafted structural fibres: a route to hierarchical fibre reinforced composites	1451
Printed circuit boards made from cellulose fibrils	1457
Sandwich type shape memory polymer composite actuators to increase the recovery moment and deformability	1465
Supercritical CO2 assisted foam extrusion for aeronautical sandwich structure manufacturing	1472
Kinetic studies and its influence on phase transition behaviour of multicomponent amine-cured epoxy blend	1480

Non-isocyanate polyurethanes based composites: a new route to sustainable fully biobased structural composites	1486
MXENE nanoparticles to impart multifunctional properties to fibre reinforced plastic composites	1495
COMBOO – properties of a novel bamboo based honeycomb core material for composite sandwich structures	1500
Effect of aspect ratio and bulk density of carbon nanotube on the electrical conductivity of polycarbonate/multi-walled carbon nanotube nanocomposites	1508
Hierarchical solutions to compressive problems in fibre-reinforced composites	1512
Tough poly(ethylene glycol)-sized bacterial cellulose sheet for high impact strength laminated acrylic composites	1518
Experimental investigation and modelling of the morphology and induced thermal properties evolution by consolidation of flax fibres hybrid reinforced thermoplastic composite	1526
Avoiding complete failure of composite t-joints by embedding sacrificial cracks inside the BONDLINE	1536
Mechanical analysis of the indentation behavior of short fiber-reinforced composites using finite element method	1542
Micro-scale measurements on epoxy using in-situ microscopic techniques	1549
Study on cure-dependent properties of epoxy molding compound and warpage of semiconductor packages	1557
Thermoplastic coating on carbon fiber for the design of sustainable composite materials	1565
Fabrication of CNT aerogel composite through reactive infiltration of polyamide 6	1571
Void reduction in graphene interlayer enhanced carbon fibre thermoplastic composites	1579
Highly deformable and processable poly(3-hydroxybutyrate) in presence of FERULIC acid-based additives	1587
Chitosan nanoparticles with ginkgo BILOBA extract in an alginate carrier as a system for the slow release of the active substance	1595

DESIGNING BICONTINUOUS SILICA-EPOXY NANOCOMPOSITES

Charles M.D. Shaw^a, David B. Anthony^b, Joseph Garguili^c, Ian Hamerton^c, Milo S.P. Shaffer^b

a: Department of Materials, Imperial College London, UK – c.shaw20@imperial.ac.uk

b: Department of Chemistry, Imperial College London, UK

c: Bristol Composites Institute, Department of Aerospace Engineering, University of Bristol, UK

Abstract: *A nanocomposite reinforced with a 3D, connected, stiff framework should offer better performance than a simple dispersion of nanoparticles. Monolithic porous silica can be used as this framework by providing a fully connected but open porous supporting skeleton for reinforcing organic polymers. Infusion of epoxy resin into silica aerogel pores may produce a bicontinuous material that more efficiently exploits the intrinsic properties of each solid phase: bicontinuous aerogel and polymer matrix component. Matrix infusion into an aerogel monolith in principle allows greater silica content than shear mixing (of particles) which is limited by aggregation and high shear viscosities. Silica content is maximised by producing aerogels of unusually high envelope density (0.2 g.cm^{-3} – 0.8 g.cm^{-3}).*

Keywords: Silica; Aerogel; Bicontinuous; Hybrid; Nanoreinforcement

1. Introduction

Epoxy resins are widely used in structural composites due to their high toughness, ease of processing, and good interfacial compatibility with reinforcing materials. However, they lack stiffness when compared to inorganic materials and some high-end thermoplastics. Silica particles dispersed within epoxy resin can improve elastic modulus without loss of toughness [1]. However, this approach increases resin viscosity which hinders processing [2], and lacks any long-range connectivity between the particles. By pre-forming a porous silica monolith, and backfilling with epoxy, a structure consisting of a fully bicontinuous, silica-epoxy network may be achieved. In this architecture, the reinforcement is evenly distributed, forming an interlocked inorganic-organic hybrid with characteristic lengthscales of less than 10 nm. The bicontinuous structure facilitates improved load transfer for greater stiffness and introduces additional failure modes for greater energy absorption [3].

Silica aerogel was chosen as the porous silica phase for this material for its simple, low-temperature synthesis and controllable mesoporosity. Pure silica aerogel is intrinsically brittle due to the weakness of interparticle neck regions in its “pearl necklace” morphology. Improved mechanical performance has been reported when the fragile network is crosslinked with organic polymers to give an X-aerogel [4]. Aerogel-based hybrids are typically made with low loadings of secondary materials to preserve the characteristic low density and thermally insulating properties of the aerogel. In this work, we aim to use the aerogel as a 3D reinforcing element in which the pores are completely backfilled with a commercially available epoxy resin, encasing the silica network as a stiff skeletal reinforcement to the epoxy. A comparison of the microstructures of the various silica-epoxy nanocomposites so far described is shown in Figure 1.

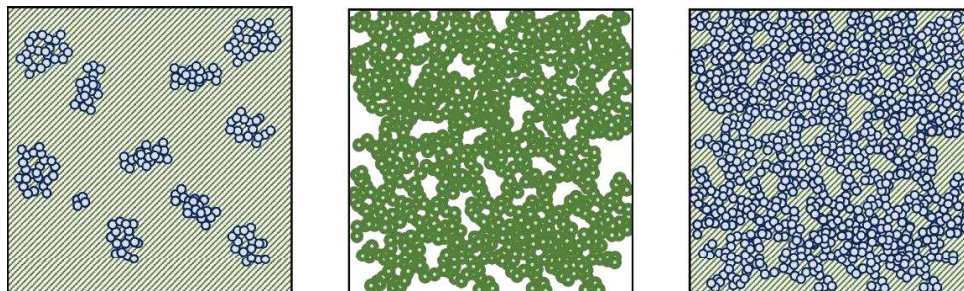


Figure 1. Cartoons depicting the microstructures of epoxy-silica nanocomposites. Left: Epoxy resin (green) reinforced with powdered silica aerogel (blue). Centre: Epoxy-crosslinked silica X-aerogel (light blue aerogel with dark green epoxy crosslinking). Right: Bicontinuous silica-epoxy hybrid monolith (blue aerogel and green epoxy).

Silica aerogel has previously been used to produce a composite polymer electrolyte by backfilling with poly(ethylene oxide) (PEO) under reduced pressures [5]. In this material, the stiff silica backbone reinforces the mechanically weak PEO enabling suppression of lithium dendrite formation. We propose that a similar vacuum technique can be applied to fill mesoporous silica monoliths with epoxy resin, combining tough epoxy with stiff silica to produce a bicontinuous composite with greater stiffness than unreinforced epoxy without loss of toughness. Silica content is maximised by producing aerogels of unusually high envelope density (0.2 g.cm^{-3} - 0.8 g.cm^{-3}). Aerogel density is restricted by the limited miscibility of siloxane precursors with water; high densities are achieved by maximising miscibility to give high siloxane concentrations. In this work, gels are dried from supercritical CO_2 to limit the influence of pore shrinkage on the final monolith density and, hence, envelope density is controlled directly from the precursor siloxane concentration. We describe the process to make such materials on a scale suitable for mechanical testing, and these tests will be conducted at a later stage.

2. Experimental

2.1 Materials

For the synthesis of silica aerogel monoliths tetramethylorthosilicate (98%, TMOS) and chlorotrimethylsilane ($\geq 98\%$, TMCS) were purchased from Sigma Aldrich, and acetone (technical grade), ethanol (absolute), water (HPLC grade), and *n*-hexane (dehydrated) were purchased from VWR. An epoxy resin with its associated hardener (Gurit Prime 27 epoxy resin and Prime Extra Slow hardener, Marineware Ltd.) were infused into the silica aerogel monoliths to produce silica-epoxy bicontinuous composites. The epoxy and hardener were mixed according to manufacturer's instructions and degassed before use. All chemicals were used as received.

2.2 Silica Aerogel Synthesis and Characterisation

Silica aerogel monoliths were produced by combining water and TMOS in a molar ratio of 24:1. This mixture was stirred for 1 h at 25°C to give a single transparent sol phase which was then poured into a mould. Cylindrical aerogel samples were cast in moulds made by machining 20 mm thick high-density polyethylene (HDPE) sheet (PE 300, Direct Plastics) on an XYZ CNC router. Gelled samples were aged for 4 days at 25°C to ensure complete reaction before exchanging from residual solvent to ethanol. Hydrophobisation of the silica surface was performed by immersion in a TMCS:*n*-hexane:ethanol mixture (1:1:8 ratio by volume). Samples were then

exchanged back to ethanol before a final exchange to acetone over 3 days. Finally, samples were dried from supercritical CO₂ using a Leica EM CPD300 critical point dryer. Envelope densities were determined by Archimedes' balance method in de-ionised water. Skeletal density was determined by helium pycnometry (Micrometrics AccuPyc II 1340). Specific surface area, pore volume, and pore radius distributions were determined from gas sorption isotherms (N₂) using a Quantachrome NOVAtouch gas sorption analyser.

2.4 Epoxy Infusion in Silica Aerogel Monoliths to Produce Composites

Silica aerogel cylinders (diameter ≈ 5.5 mm, length ≈ 15 mm) were backfilled with epoxy by immersion in epoxy resin/hardener mixture under reduced pressure. The chosen commercially available resin system has low viscosity (170 cP to 180 cP at 25 °C) and long vacuum flow time (7 h 40 min at 25 °C). Owing to their fragility, aerogel monoliths were supported in heat-shrink tubing during infusion. Once immersed, the entire system was evacuated to 1 mbar in a vacuum oven for 6 h at 25 °C.

2.5 Composite Characterisation

The degree of infusion of epoxy into the porous silica structure was quantified as a backfill volume percentage (β) using Equation (1),

$$\beta = \frac{\Delta\rho_b}{\varphi \cdot \rho_e} \quad (1)$$

where $\Delta\rho_b$ is the difference in envelope density between the unmodified silica aerogel monolith and the epoxy-infused silica aerogel monolith, φ is the porosity of the silica aerogel monolith, and ρ_e is the cured epoxy density determined by Archimedes' balance method. The change in morphology following epoxy backfilling is observed by scanning electron microscopy using a LEO Gemini 1525 FEG SEM set at 5 kV with In lens detector.

3. Results and Discussion

The silica aerogel synthesis employed here was designed for scalability and processability. TMOS was chosen for its ability to react with water and self-mix from an initially biphasic liquid by evolving methanol without the need for additional solvents or catalysts. This miscibility is higher than that for alternative orthosilicates facilitating the formation of aerogels with higher bulk density giving a higher loading of silica reinforcement in the silica-epoxy composite. Samples were dried from supercritical CO₂ to eliminate capillary pressures resulting from solvent evaporation. This process minimises pore collapse which would otherwise result in increased envelope density and smaller pore radii which may inhibit infusion of epoxy. Samples were hydrophobised by reacting TMCS with surface silanol (OH) groups. This treatment was performed for the following reasons:

- Hydrophilic (non TMCS-treated) samples formed in this work were found to fracture in the presence of ambient moisture.
- Hydrogen bonded water molecules would be difficult to remove ahead of epoxy infusion. This residual water could affect the epoxy cure and produce voids in the composite structure.
- Furthermore, functionalisation with trimethylsilyl groups prevents silanol groups from reacting chemically with epoxy resin or hardener. This reaction may alter the

stoichiometry of the epoxy resin/hardener mixture. Silica-epoxy bi-continuous materials with a designed covalent interface will nevertheless be explored in future work.

Density and pore structure characteristics for the silica aerogel are summarised in Table 1. The BJH pore size distribution indicates that most of the porosity comprises mesopores with radii between 2 nm and 3.2 nm (Figure 2). The large specific surface area of silica aerogel (951 m².g⁻¹) results in an equally large silica-epoxy interface. This may increase the toughness of the material through crack pinning and deflection. Dry silica aerogel monoliths were translucent and bluish in colour due to Rayleigh scattering in the porous structure (Figure 3). Following epoxy infusion, the composite was uniform in appearance with greater transparency than uninfused aerogel (Figure 3) due to reduced scattering and closer matching of refractive indices [5]. Once cured, excess epoxy was removed, and the dimensions of the cylinder were measured to ensure that only the epoxy-silica composite remained. The mean backfill vol.%, $\beta = 99.3\%$ was calculated for six samples using Eq. (1) as summarised in Table 2. This value indicates that infusion of liquid epoxy into the porous epoxy structure was almost complete. Scanning electron microscopy images show the filling of pores by epoxy (Figure 4).

Table 1: Silica aerogel monolith properties where ρ_b is envelope density, ρ_s is skeletal density, SSA is specific surface area, r_{pore} is mean pore radius and V_{pore} is pore volume.

ρ_b (g.cm ⁻³)	ρ_s (g.cm ⁻³)	SSA (m ² .g ⁻¹)	r_{pore} (nm)	V_{pore} (cm ³ .g ⁻¹)
0.226 ± 0.009	1.50 ± 0.02	951 ± 25	2.60 ± 0.17	3.81 ± 0.25

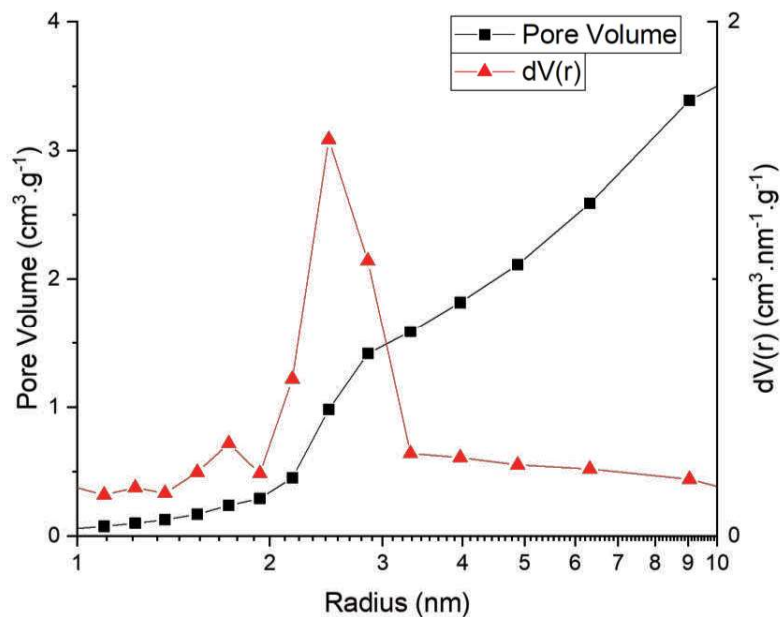


Figure 2: BJH plot calculated from silica aerogel gas sorption isotherm with the differential with respect to the pore radius included.

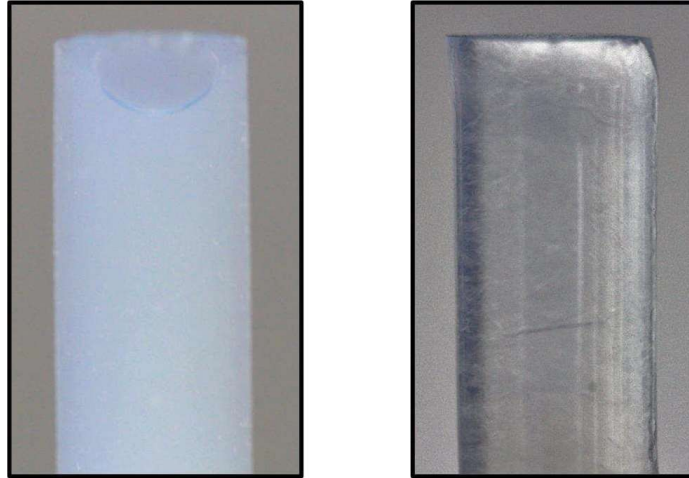


Figure 3: Photograph of silica aerogel monolith (left) and epoxy-infused silica aerogel monolith (right).

Table 2: Summary of composition of bicontinuous silica-epoxy material. Uncertainty is given as one standard deviation.

ρ_f (g.cm ⁻³)	Backfill vol.%	Void vol.%	Silica wt.%	Epoxy wt.%
1.189 ± 0.016	99.3 ± 1.9	0.6 ± 1.6	18.5 ± 0.7	81.5 ± 0.7

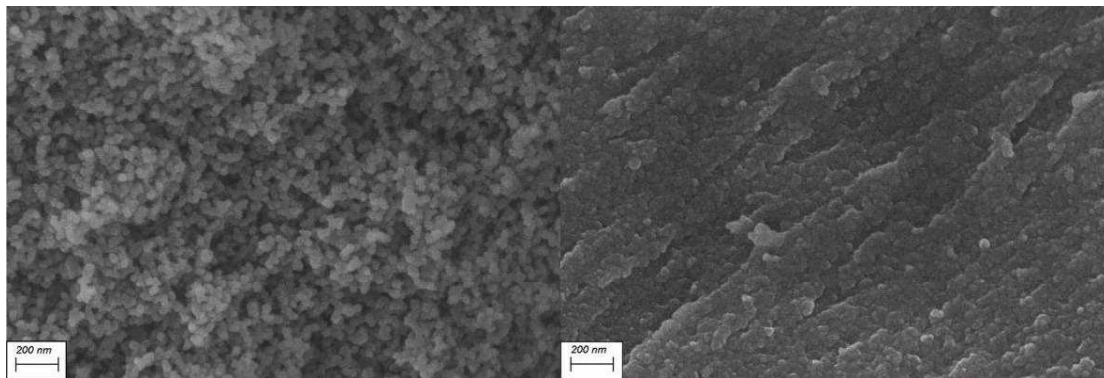


Figure 4: Scanning electron micrographs for silica aerogel before (left) and after (right) infusion with epoxy resin.

4. Conclusions

A silica-epoxy inorganic-organic bicontinuous hybrid composite material has been produced by backfilling mesoporous monolithic silica aerogel with liquid epoxy resin. Backfill vol.% was calculated from pre- and post-infusion envelope densities and indicated that 99.3 pore vol.% was filled resulting in a void content of 0.6 vol.%. This low void content shows that silica pores with radii of 2.0 nm - 3.2 nm uptake liquid epoxy resin. The resulting composite has a continuous 3D silica reinforcement which will provide the epoxy resin with improved stiffness by facilitating long range load transfer. Pre-forming the silica network as a monolithic structure also enables

high weight loadings of reinforcement without incurring the high viscosities seen in dispersed particulate systems. A simple two component silica aerogel synthesis has been employed which could enable modification of precursor composition to produce higher silica aerogel envelope densities leading to a higher silica content in the bicontinuous composite. Future work will test monolithic samples in compression to determine the optimum silica content for improved mechanical performance. Higher silica volume fractions could also be achieved through application of a lower porosity aerogel with a larger mean pore radius. Such a material may be achieved through selection of appropriate alternative monomers and catalysts or application of templating techniques. This material is currently limited to small scale test samples due to the geometric limitations imposed by critical point drying. Large scale structural elements will require the use of mesoporous silica materials which are stable to ambient pressure drying.

Acknowledgements

The authors kindly acknowledge the funding for this research provided by UK Engineering and Physical Sciences Research Council (EPSRC) programme Grant EP/T011653/1, Next Generation Fibre-Reinforced Composites: a Full Scale Redesign for Compression in collaboration with University of Bristol.

5. References

1. Salimian S, Zadhoush A. Water-glass based silica aerogel: unique nanostructured filler for epoxy nanocomposites. *Journal of Porous Materials*. 2019; 26(6):1755-65.
2. Rahatekar SS, Koziol KKK, Butler SA, Elliott JA, Shaffer MSP, Mackley MR, *et al*. Optical microstructure and viscosity enhancement for an epoxy resin matrix containing multiwall carbon nanotubes. *Journal of Rheology*. 2006; 50(5):599-610.
3. Quaresimin M, Schulte K, Zappalorto M, Chandrasekaran S. Toughening mechanisms in polymer nanocomposites: From experiments to modelling. *Composite Science and Technology*. 2016; 123:187-204.
4. Meador MAB, Fabrizio EF, Ilhan F, Dass A, Zhang G, Vassilaras P, *et al*. Cross-linking Amine-Modified Silica Aerogels with Epoxies: Mechanically Strong Lightweight Porous Materials. *Chemistry of Materials*. 2005; 17(5):1085-98.
5. Lin D, Yuen PY, Liu Y, Liu W, Liu N, Dauskardt RH, *et al*. A Silica-Aerogel-Reinforced Composite Polymer Electrolyte with High Ionic Conductivity and High Modulus. *Advanced Materials*. 2018; 30(32):1802661.